



Water diffusion coefficients during copper electropolishing

BING DU¹ and IAN IVAR SUNI^{2*}

¹Department of Chemistry, Center for Advanced Materials Processing, Clarkson University, Potsdam, NY 13699-5705, USA

²Department of chemical Engineering, Centre for Advanced Materials Processing, Clarkson University, Potsdam, NY 13699-5705, USA

(*author for correspondence, e-mail: isuni@clark.edu)

Received 19 March 2004; accepted in revised form 23 June 2004

Key words: chronoamperometry, cottrell analysis, diffusion coefficient, electrodisolution, electropolishing, Levich analysis, planarization

Abstract

Cu electropolishing was studied using a rotating disc electrode in a variety of phosphoric acid-based electrolytes, including several with ethanol and other species added as diluents. Diluents allow a wider range of water concentrations and electrolyte viscosities to be accessed and also reduce the removal rate during Cu electropolishing, simplifying possible application to damascene processing. Transient and steady state currents in the mass transfer limited regime are shown to depend on both the number of water acceptor molecules associated with each dissolving Cu ion and on the effective diffusion coefficient of water. Transient analysis samples the bulk transport properties, whereas steady state analysis integrates them through the diffusion layer. Assuming that the effective diffusion coefficients appropriate to transient and steady state behavior are the same, about one water molecule is associated with each dissolving Cu ion. This analysis yields effective diffusion coefficients for water on the order of 10^{-9} cm² s⁻¹. However, the data is also consistent with an assumption that six water molecules are associated with each dissolving Cu ion, but the effective diffusion coefficient appropriate for a Levich analysis is somewhat lower than that in the bulk electrolyte. This analysis yields effective diffusion coefficients for water on the order of 10^{-8} – 10^{-7} cm² s⁻¹. The latter interpretation, that six water molecules are associated with each dissolving Cu ion, appears more likely since it provides almost exact agreement with the effective diffusion coefficient reported previously by Vidal and West. In combination with previously published impedance results ruling out a salt film mechanism, the good agreement between the transient and steady state analyses confirm that water is the acceptor species that complexes dissolving Cu ions in phosphoric acid-based electropolishing baths.

1. Introduction

Cu electropolishing has recently been proposed for surface planarization following Cu electroplating during damascene processing of Si-based semiconductor devices [1–5]. While local planarization occurs through the action of the electropolishing electrolyte, global planarization is more difficult. One common approach to global planarization is the use of a rotating wafer/electrode configuration (RDE) for simultaneous Cu removal across the wafer surface [1, 2, 5]. This approach provides rapid Cu removal, but suffers from the drawback that surface features of varying size, such as those created by Cu electrodeposition from superfilling additives, may be difficult to planarize simultaneously. Additive-containing baths have been proposed to address this problem [4], but their performance has not yet been widely validated. Another approach involves use of a scanning cathode or segmented cathode configuration [6]. While this approach is more

flexible for surfaces with significant topography, the net removal rate will be much lower. Other challenges to commercialization include island formation due to a loss of contact when the remaining Cu film becomes quite thin. Advantages relative to chemical mechanical planarization (CMP) include simplicity, cost-of-ownership, easier endpoint detection, particle contamination is not introduced, and better compatibility with porous low-*k* dielectrics, which are mechanically fragile and may be damaged during CMP [4].

In addition, Cu electropolishing in phosphoric acid electrolytes has been a prototype for fundamental studies of electropolishing [7–13]. Despite intensive investigation, the identity of the solution phase species involved in the rate-determining step remains controversial, with some groups proposing phosphate-containing species and others water [5, 7, 10, 12]. Such knowledge may be important for commercial application to damascene processing of Si wafers, since this will determine the removal rate that is obtained. We recently

reported Levich analyses of the limiting current densities in a variety of phosphoric acid-based Cu electropolishing electrolytes that establish water as the likely acceptor species [14]. These results include electrolytes with ethanol and other diluents added, which allows one to obtain lower limiting current densities, preventing rapid Cu film removal during damascene processing. In this report, we present the results of transient and steady state analyses of Cu electropolishing in phosphoric acid-based electrolytes extending to lower water concentrations.

2. Experimental details

Experiments were performed on 5 mm diameter standard Cu rotating disc electrodes (RDE) from Pine Instruments. For all electrochemistry experiments, a saturated calomel (SCE) reference electrode and a Pt wire counter electrode were employed in a standard three-electrode geometry, controlled with a EG&G PAR model 263 A-1 potentiostat/galvanostat. Most of the electrolytes were prepared from 85 wt% phosphoric acid (J.T. Baker) and analytical grade diluents, including water, methanol and ethanol. The three electrolytes with the lowest water concentration were prepared from 105% w/w polyphosphoric acid (Rhodia). The actual phosphoric acid concentration of these two reagents was determined by dilution and subsequent acid–base titration.

The electrolyte viscosities were measured with a Brookfield Synchro-lectric viscometer, and the electrolyte density was measured by weighing the electrolyte in a volumetric flask. The variation of repeat viscosity measurements is about 1.5%. Unless otherwise indicated, all experiments were performed at room temperature ($22 \pm 1^\circ\text{C}$). Most of the reported diffusion coefficients were verified by repeated experiments, with typical variations in limiting current densities of about 4%, and typical variations in the slope of the initial current–time transient of about 15%.

3. Results and discussion

Figure 1 shows a cyclic voltammogram for 17.7 M H_2O and 13.3 M H_3PO_4 at a scan rate of 10 mV s^{-1} , showing little noise in the limiting current density plateau. Subsequent studies involve a variety of different H_3PO_4 -based electrolytes, including many to which diluents such as ethanol have been added. These diluents allow a wider range of water concentrations and electrolyte viscosities to be accessed. They also reduce the removal rate during Cu electropolishing, simplifying possible application to damascene processing. These diluents have been chosen to be electrochemically much less active than H_3PO_4 and H_2O and less likely to complex Cu^{2+} , although neither assumption has been rigorously verified.

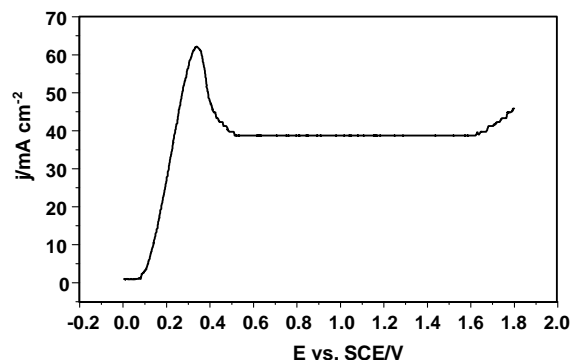


Fig. 1. Polarization curve for 17.7 M H_2O and 13.3 M H_3PO_4 at 240 rpm and a scan rate of 10 mV s^{-1} .

Figure 2 shows the current transients obtained in three different phosphoric acid-based electrolytes following a potential step from a potential at which the current is zero to a potential in the mass transfer-limited regime. Each of these curves eventually reaches a steady state value, the limiting current density, at times greater than those shown in Figure 2. At least two quantities, the initial slope of the current–time relationship, which can be analyzed by the Cottrell equation, and the steady state current, which can be analyzed using the Levich equation, can be obtained from each current transient. However, knowledge of the rate-determining species is needed.

As mentioned in the Introduction, both the mechanism and the acceptor species during Cu electropolishing in phosphoric acid-based electrolytes are somewhat controversial. This analysis will initially assume that Cu electropolishing is rate-limited by diffusion of water, assumed to be the acceptor species for dissolving Cu ions. Subsequent analysis provides supporting evidence for this claim, which will then be discussed in more detail. A complication of this system is that transport phenomena control the formation of the diffusion layer, while the measured current scales inversely with the degree of complexation. In such a system, a Levich analysis yields [12, 15],

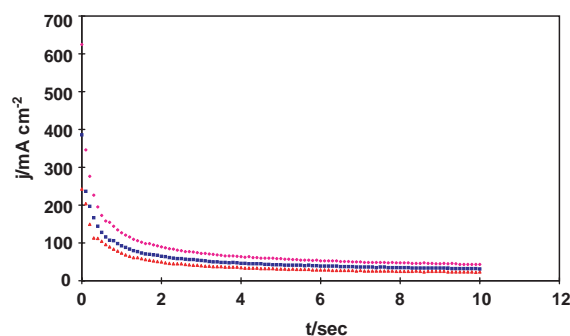


Fig. 2. Current transients recorded at 240 rpm for 17.7 M H_2O and 13.3 M H_3PO_4 (\blacklozenge), for 12.3 M H_2O and 12.3 M H_3PO_4 and 2.7 M $\text{C}_2\text{H}_5\text{OH}$ (\blacksquare), and for 7.8 M H_2O and 10.1 M H_3PO_4 , and 6.2 M $\text{C}_2\text{H}_5\text{OH}$ (\blacktriangle).

$$j_{\text{lim}} = \frac{1.24}{S_{\text{H}}} F D_{\text{H}}^{2/3} \omega^{1/2} \nu^{-1/6} C_{\text{H}} \quad (1)$$

where j_{lim} is the limiting current density, S_{H} is the ratio of water acceptor ions for every dissolving Cu^{2+} ion, D_{H} is the effective diffusion coefficient of water, C_{H} is the bulk water concentration, and the other symbols have their usual meaning. Similarly, a Cottrell analysis yields, [15]

$$j(t) = \frac{2FD_{\text{H}}^{1/2}C_{\text{H}}}{S_{\text{H}}\pi^{1/2}t^{1/2}} \quad (2)$$

It should be noted that the effective diffusion coefficients for water (D_{H}) need not be the same in these two equations. Cottrell analysis provides a value for the effective diffusion coefficient at the bulk composition and viscosity, while Levich analysis provides a value integrated through the diffusion layer. This can be seen most easily through the variation in the viscosity with water concentration, which suggests that the viscosity at the water-depleted interface may be nearly an order of magnitude greater than the viscosity in the bulk electrolyte (B.Du and I.I Suri, unpublished results). Simple Stokes–Einstein arguments then suggest that the effective diffusion coefficient near the interface might be considerably lower than that in the bulk electrolyte. For this reason, simultaneous solution of the Levich and Cottrell equations to obtain S_{H} and D_{H} might be a mistake.

Figure 3 shows Cottrell plots for the same electrolytes whose current transients are shown in Figure 2. Table 1 provides the composition, density, and kinematic viscosity determined for each phosphoric acid-based electrolyte. In addition, Table 1 contains the ratio $D_{\text{H}}^{1/2}/S_{\text{H}}$ determined from a Cottrell analysis and the ratio $D_{\text{H}}^{2/3}/S_{\text{H}}$ determined from a Levich analysis. The last four columns in Table 1 provide the effective diffusion coefficients for water for two extreme cases, values of one and six for S_{H} . The former value provides the best agreement between the effective diffusion coefficients obtained from the Levich and Cottrell analyses, while the latter value corresponds to that expected in the bulk electrolytes.

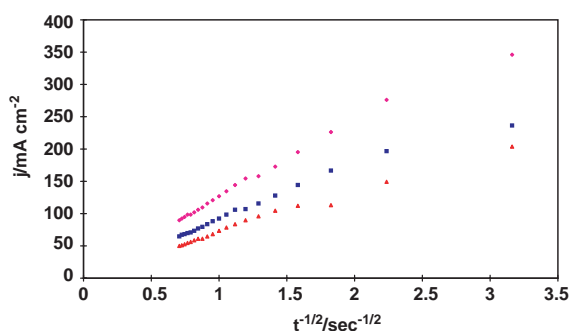


Fig. 3. Cottrell analysis of the current transients from Figure 2, for $t < 2$ s.

Assuming a value of one for s_{H} yields diffusion coefficients in the $10^{-9} \text{ cm}^2 \text{ s}^{-1}$ range, while assuming a value of six yields values in the 10^{-8} – $10^{-7} \text{ cm}^2 \text{ s}^{-1}$ range, with the Levich analysis typically yielding lower diffusion coefficients than the Cottrell analysis. This would suggest that the diffusion coefficient is lower near the surface than in the bulk electrolyte. While this might be expected for this highly dehydrated region from Stokes–Einstein arguments, concentrated phosphoric acid does not appear to be a hydrodynamically simple fluid, as discussed below. In addition, given the wide difference between the bulk and near surface electrolyte viscosity, the Stokes–Einstein equation would predict an even larger difference between the effective diffusion coefficients from the Levich and Cottrell analyses than is actually observed.

The only reported value for an effective diffusion coefficient for water in phosphoric acid-based electrolytes is the estimate of $5 \times 10^{-8} \text{ cm}^2 \text{ sec}^{-1}$ obtained by Vidal and West from electrohydrodynamic (EHD) impedance measurements [12], which are independent of the value of S_{H} . This technique actually determines the Schmidt number, with the effective diffusion coefficient then determined using the bulk viscosity. They report an effective diffusion coefficient for water in 85 wt% H_3PO_4 , which corresponds to the electrolyte composition in Table 1 of 15.2 M H_3PO_4 and 11.7 M H_2O . If one chooses a value of six for s_{H} , the current result of $5.2 \times 10^{-8} \text{ cm}^2 \text{ s}^{-1}$ agrees exactly with that reported by Vidal and West to within the number of significant figures that were reported.

Regardless of the value assumed for S_{H} , the effective diffusion coefficients obtained in Table 1 from both transient (Cottrell) and steady state (Levich) analyses are remarkably invariant to electrolyte composition. For example, although the water concentration varies from 4.03 to 20.0 M, for transient analysis with an assumed value of six for s_{H} , the effective diffusion coefficients of water reported in Table 1 vary only from 1.1 to $3.0 \times 10^{-7} \text{ cm}^2 \text{ s}^{-1}$. This is quite surprising given the widely varying diluent concentrations and the variation of almost an order of magnitude in electrolyte viscosity.

However, previous authors have noted that the transport properties of concentrated phosphoric acid are anomalous, and they have suggested that transport cannot be described by the prototypical hydrodynamic model of slip-free particle motion through a liquid, or in other words, by the Stokes–Einstein equation [16, 17]. For example, concentrated phosphoric acid electrolytes have unusually high conductivity given their high viscosity. In addition, diffusion coefficient measurements for both protons and phosphorus-containing species exhibit unusual concentration and temperature dependence [16, 17]. The relative invariance with electrolyte composition of the diffusion coefficients in Table 1 reinforces the conclusion that concentrated phosphoric acid is not a hydrodynamically simple fluid.

Fundamental reasons exist that suggest S_{H} is unlikely to have a value of six throughout the diffusion layer. In

Table 1. Composition, density, kinematic viscosity, and effective diffusion coefficients ($\text{cm}^2 \text{ s}^{-1}$) determined for each electrolyte

Composition	ρ g cm^{-3}	ν $\text{cm}^2 \text{ s}^{-1}$	j_{lim} mA cm^{-2}	$D^{1/2}_{\text{H}}/S_{\text{H}}$ (Cottrell)	$D^{2/3}_{\text{H}}/S_{\text{H}}$ (Levich)	D_{H} (Cot) ($S_{\text{H}} = 1$)	D_{H} (Lev) ($S_{\text{H}} = 1$)	D_{H} (Cot) ($S_{\text{H}} = 6$)	D_{H} (Lev) ($S_{\text{H}} = 6$)
17.9 M H_3PO_4 + 4.03 M H_2O	1.828	1.028	6.17	7.45×10^{-5}	2.57×10^{-6}	5.6×10^{-9}	4.1×10^{-9}	2.0×10^{-7}	6.0×10^{-8}
17.0 M H_3PO_4 + 6.90 M H_2O	1.790	0.641	8.54	6.23×10^{-5}	1.92×10^{-6}	3.9×10^{-9}	2.7×10^{-9}	1.4×10^{-7}	3.9×10^{-8}
15.8 M H_3PO_4 + 10.6 M H_2O	1.742	0.475	12.3	5.49×10^{-5}	1.71×10^{-6}	3.0×10^{-9}	2.2×10^{-9}	1.1×10^{-7}	3.3×10^{-8}
15.2 M H_3PO_4 + 11.7 M H_2O	1.702	0.286	20.0	6.23×10^{-5}	2.32×10^{-6}	3.9×10^{-9}	3.5×10^{-9}	1.4×10^{-7}	5.2×10^{-8}
13.3 M H_3PO_4 + 17.7 M H_2O	1.621	0.163	34.4	6.42×10^{-5}	2.40×10^{-6}	4.1×10^{-9}	3.7×10^{-9}	1.5×10^{-7}	5.5×10^{-8}
12.5 M H_3PO_4 + 20.0 M H_2O	1.587	0.137	46.2	7.06×10^{-5}	2.77×10^{-6}	5.0×10^{-9}	4.6×10^{-9}	1.8×10^{-7}	6.8×10^{-8}
13.5 M H_3PO_4 + 17.0 M H_2O + 0.1 M CuSO_4	1.642	0.187	31.0	7.69×10^{-5}	2.30×10^{-6}	5.9×10^{-9}	3.5×10^{-9}	2.1×10^{-7}	5.1×10^{-8}
13.2 M H_3PO_4 + 17.5 M H_2O + 0.26 M CuSO_4	1.649	0.195	32.7	7.63×10^{-5}	2.37×10^{-6}	5.8×10^{-9}	3.6×10^{-9}	2.1×10^{-7}	5.4×10^{-8}
13.5 M H_3PO_4 + 16.0 M H_2O + 0.53 M CuSO_4	1.697	0.265	23.6	6.34×10^{-5}	1.97×10^{-6}	4.0×10^{-9}	2.8×10^{-9}	1.5×10^{-7}	4.1×10^{-8}
10.1 M H_3PO_4 + 7.8 M H_2O + 6.2 M $\text{C}_2\text{H}_5\text{OH}$	1.417	0.280	17.1	8.15×10^{-5}	2.96×10^{-6}	6.6×10^{-9}	5.1×10^{-9}	2.4×10^{-7}	7.5×10^{-8}
10.8 M H_3PO_4 + 8.3 M H_2O + 5.3 M $\text{C}_2\text{H}_5\text{OH}$	1.456	0.277	18.0	7.98×10^{-5}	2.92×10^{-6}	6.4×10^{-9}	5.0×10^{-9}	2.3×10^{-7}	7.3×10^{-8}
12.4 M H_3PO_4 + 9.5 M H_2O + 3.5 M $\text{C}_2\text{H}_5\text{OH}$	1.541	0.276	18.5	6.89×10^{-5}	2.62×10^{-6}	4.7×10^{-9}	4.2×10^{-9}	1.7×10^{-7}	6.2×10^{-8}
12.3 M H_3PO_4 + 12.3 M H_2O + 2.7 M $\text{C}_2\text{H}_5\text{OH}$	1.547	0.238	23.8	6.66×10^{-5}	2.54×10^{-6}	4.4×10^{-9}	4.0×10^{-9}	1.6×10^{-7}	5.9×10^{-8}
12.3 M H_3PO_4 + 15.1 M H_2O + 1.8 M $\text{C}_2\text{H}_5\text{OH}$	1.559	0.185	31.0	6.49×10^{-5}	2.59×10^{-6}	4.2×10^{-9}	4.2×10^{-9}	1.5×10^{-7}	6.1×10^{-8}
11.9 M H_3PO_4 + 16.6 M H_2O + 1.3 M Glycerol	1.580	0.234	28.6	6.49×10^{-5}	2.26×10^{-6}	4.2×10^{-9}	3.4×10^{-9}	1.5×10^{-7}	5.0×10^{-8}
12.1 M H_3PO_4 + 14.7 M H_2O + 2.0 M Ethylene Glycol	1.578	0.222	27.9	6.58×10^{-5}	2.46×10^{-6}	4.3×10^{-9}	3.9×10^{-9}	1.6×10^{-7}	5.7×10^{-8}
11.6 M H_3PO_4 + 8.9 M H_2O + 6.5 M CH_3OH	1.500	0.219	22.6	9.13×10^{-5}	3.28×10^{-6}	8.3×10^{-9}	5.9×10^{-9}	3.0×10^{-7}	8.7×10^{-8}

addition to the likelihood for variation of the effective diffusion coefficient within the diffusion layer, one must consider the likelihood of variation in the Cu–water complexation equilibria. Since the Cu^{2+} concentration is at a maximum, while the water concentration is at a minimum, S_{H} is likely quite low at the interface. On the other hand, S_{H} might reach the expected value of six in the bulk electrolyte. In addition, steric constraints at the interface suggest that six water molecules cannot coordinate one Cu ion.

One can indirectly address the possibility of variation in the effective diffusion coefficient of water during formation of the diffusion layer by an alternative analysis of the current transients shown in Figure 2. Theoretical treatments of the current transient at a rotating disc electrode following application of a potential step into the mass transfer-limited regime have been published by several authors [18–22]. The present study will follow the formalism originally published by Bruckenstein and Prager [20], but corrected slightly by Myers et al [21]. to yield proper values at the Cottrell limit (short time) and the Levich limit (long time). Assuming a linear concentration gradient within the diffusion layer, the convective diffusion equation can be solved using the Method of Moments to yield: [20, 21]

$$t = 0.2122 \frac{\delta_{\text{SS}}^2}{D_{\text{H}}} \left\{ \frac{1}{2} \ln \left[\frac{1-R^3}{(1-R)^3} \right] - \sqrt{3} \tan^{-1} \left(\frac{\sqrt{3}R}{R+2} \right) \right\} \quad (3)$$

Here $R=j_{\text{SS}}/j$ is the ratio of the steady state current to the instantaneous current and δ_{SS} is the steady state (Levich) diffusion layer thickness. Although this formalism has been criticized because an explicit form is not given for the current as a function of time, this equation has been shown to be accurate to within 1–2% [22].

In addition, because the dependent variable is a current ratio, this result does not depend on either the stoichiometric number of electrons transferred ($n = 2$) or the number of acceptor species per Cu ion (S_{H} =unknown). Similarly, one can show that the steady state value of the diffusion layer thickness (δ_{SS}), which is known to be independent of n , is also independent of S_{H} . This equation can also be written as:

$$t = 0.2122 \frac{\delta_{\text{SS}}^2}{D_{\text{H}}} f(R) \quad (4)$$

This allows elegant determination of the effective diffusion coefficient from the slope of $f(R)$ versus time. However, it should be noted that the steady state diffusion layer thickness varies with $D_{\text{H}}^{1/3}$, where this value is again integrated through the diffusion layer. In addition, it is unclear whether the value of D_{H} explicitly included in Equation (4) corresponds to a bulk or near-

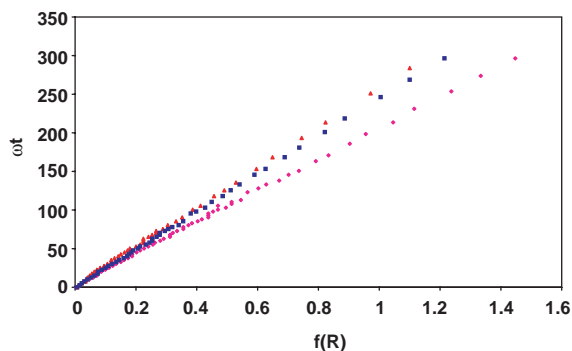


Fig. 4. Full fit to Equation (4) for the current transients from Figure 2.

surface diffusion coefficient. Lastly, data fits to Equation (4) were not found to be very accurate at long times ($R \rightarrow 1$) due both to the functional form of $f(R)$ and to the strong sensitivity to the exact choice of the limiting current density.

For these reasons, rather than using Equation (4) to determine effective diffusion coefficients, this will be employed to approximate the extent to which the effective diffusion coefficient varies during each experiment. Figure 4 shows the current transients from Figure 2 fit to Equation (4). Such plots consistently show little curvature as t increases during the experiment. One might expect such curvature if the effective diffusion coefficient for water changes during diffusion layer formation. However, given the highly nonlinear form of Equation (3), this argument is somewhat indirect.

Thus the current results can be interpreted in two different ways. If one assumes that the effective diffusion coefficient for water is approximately constant within the diffusion layer, S_H is approximately one, and the effective diffusion coefficient is in the $10^{-9} \text{ cm}^2 \text{ s}^{-1}$ range. This interpretation is consistent with the lack of curvature seen in Figure 4 and with the low concentration of water near the interface, which suggests a low value of S_H , but is inconsistent with the diffusion coefficient reported by Vidal and West. Alternatively, if one assumes a value of six for S_H , the results are consistent with those of Vidal and West and with spectrophotometry experiments that indicate little change in the absorption near 900 nm, which is associated with the formation of $\text{Cu}(\text{H}_2\text{O})_6^{2+}$ (B. Du and I. I. Suni, unpublished results). In this case the effective water diffusion coefficient in the bulk electrolyte is in the 10^{-8} – $10^{-7} \text{ cm}^2 \text{ s}^{-1}$ range, and the effective water diffusion coefficient is somewhat lower when integrated through the diffusion layer than for the bulk electrolyte. We currently favor the latter interpretation that S_H is likely six.

Regardless of the true value of S_H , the effective diffusion coefficients obtained from the Levich and Cottrell analyses are in good agreement, providing further evidence that water diffusion is indeed the rate-limiting step during Cu electropolishing in phosphoric acid electrolytes. Even if one assumes that the effective

water diffusion coefficient obtained from the Cottrell and Levich analyses is different, and the value for S_H (six) is chosen that maximizes this difference, the variation in diffusion coefficients is relatively small throughout the last column of Table 1, which contains a wide range of water concentrations. Such a result would be quite fortuitous if water were not the rate-determining, acceptor species. However, this does not mean that the dissolving Cu ion complexes do not also include phosphate-containing species. It should be noted the previously published impedance analysis by Vidal and West shows that both the ohmic resistance and double layer capacitance are independent of both the applied potential and rotational speed [12]. This demonstrates convincingly that a salt film precipitation mechanism does not apply to Cu electropolishing in phosphoric acid based electrolytes.

Acknowledgements

This research has been supported by the Center for Advanced Materials Processing (CAMP) at Clarkson University and by National Science Foundation Grant # CTS-0094773.

References

1. R.J. Contolini, A.F. Bernhardt and S.T. Mayer, *J. Electrochem. Soc.* **141** (1994) 2503.
2. R.J. Contolini, S.T. Mayer, R.T. Graff, L. Tarte and A.F. Bernhardt, *Solid State Technol.* **10**(6) (1997) 155.
3. S.C. Chang, J.M. Shieh, C.C. Huang, B.T. Dai and M.S. Feng, *Jap. J. Appl. Phys.* **1** **41** (2002) 7332.
4. S.C. Chang, J.M. Shieh, B.T. Dai, M.S. Feng, Y.H. Li, C.H. Shih, M.H. Tsai, S.L. Shue, R.S. Liang and Y.L. Wang, *Electrochem. Solid-State Lett.* **6** (2003) G72.
5. D. Padhi, J. Yahalom, S. Gandikota and G. Dixit, *J. Electrochem. Soc.* **150** (2003) G10.
6. H. Wang, U.S. Patent # 6,395,152.
7. J. Edwards, *J. Electrochem. Soc.* **100** (1953) 189C.
8. J. Edwards, *J. Electrochem. Soc.* **100** (1953) 223C.
9. T.P. Hoar and G.P. Rothwell, *Electrochim. Acta* **9** (1964) 135.
10. S.H. Glarum and J.H. Marshall, *J. Electrochem. Soc.* **132** (1985) 2872.
11. S.H. Glarum and J.H. Marshall, *J. Electrochem. Soc.* **132** (1985) 2878.
12. R. Vidal and A.C. West, *J. Electrochem. Soc.* **142** (1995) 2682.
13. R. Vidal and A.C. West, *J. Electrochem. Soc.* **142** (1995) 2689.
14. B. Du and I.I. Suni, *J. Electrochem. Soc.* **151** (2004) C375.
15. A.J. Bard and L.R. Faulkner, 'Electrochemical Methods' 2nd edn (John Wiley & Sons, New York, 2001).
16. H. Chakrabarti, *J. Phys. Condens. Matt.* **8** (1996) 7019.
17. S.H. Chung, S. Bajue and S.G. Greenbaum, *J. Chem. Phys.* **112** (2000) 8515.
18. R.P. Buck and H.E. Keller, *Anal. Chem.* **35** (1963) 400.
19. V. Yu. Filinovskii and V.A. Kiryanov, *Dokl. Akad. Nauk.* **156** (1964) 1412.
20. S. Bruckenstein and S. Prager, *Anal. Chem.* **39** (1967) 1161.
21. D.J. Myers, R.A. Osteryoung and J. Osteryoung, *Anal. Chem.* **46** (1974) 2089.
22. K. Viswanathan and H.Y. Cheh, *J. Appl. Electrochem.* **9** (1979) 537.